

## Temperature Dependence of the Polarizability of Sodium Clusters

S. A. Blundell, C. Guet, and Rajendra R. Zope

*Département de Recherche Fondamentale sur la Matière Condensée, CEA Grenoble, 17 rue des Martyrs,  
F-38054 Grenoble Cedex 9, France*

(Received 25 February 2000)

We calculate the static dipole polarizability at finite temperature of sodium clusters of size 8, 20, 40, 55, 93, and 139 using an extended Thomas-Fermi description of the valence electrons. We find polarizabilities at 300 K that are roughly 15% greater than at 0 K, consistent with discrepancies between theoretical polarizabilities at 0 K and measured polarizabilities. We predict that a sharp rise in the polarizability, of about 5%, occurs for sizes of 55 and 139 when the cluster melts, offering the possibility of an alternative method for measuring cluster melting points.

PACS numbers: 36.40.Cg, 31.15.Ew, 31.15.Qg, 36.40.Ei

The polarizabilities of small clusters of sodium and potassium up to size  $N = 40$  were first measured in 1984 by Knight *et al.* [1] in one of the earliest experiments on free (unsupported) metallic clusters. They found polarizabilities that (depending on the cluster size  $N$ ) were from 30% to 100% larger than the classical polarizability  $\alpha_{cl} = R_b^3$  of a perfectly conducting sphere of radius  $R_b = r_s N^{1/3}$ , where  $r_s$  is the bulk Wigner-Seitz radius. Part of this discrepancy could be explained as a finite-size effect. Jellium-model calculations [2] in which the  $\text{Na}^+$  or  $\text{K}^+$  ions in the cluster were replaced by a uniformly charged sphere of radius  $R_b$  gave an enhanced polarizability  $\alpha_{jel} = (R_b + \delta)^3$ , where  $\delta \sim 1a_0$  could be interpreted as due to the “spillout” of electrons beyond the surface of the jellium sphere. But  $\alpha_{jel}$  was generally still smaller than the experimental polarizability. Since then, more sophisticated calculations [3–10] of the polarizability at 0 K that retain the full three-dimensional ionic structure of the cluster, and new measurements [10–12] of the polarizabilities of alkali-metal clusters, have confirmed a general trend in which (at least for  $N \geq 8$ ) theoretical polarizabilities at 0 K are slightly smaller than the measured polarizabilities.

This discussion neglects the role of finite temperature, which would be expected to increase the cluster volume and, hence, its polarizability. Indeed, while in existing experiments the clusters were not well thermalized and their temperature was not well known, conditions were such that temperatures of several hundred degrees Kelvin were to be expected. It has recently become possible to control the cluster temperature rather precisely [13], and it may soon be possible to measure the polarizability as a function of temperature [14]. In this Letter we estimate, for the first time, the temperature dependence of the polarizability of sodium clusters in the size range  $N = 8$ –139 by averaging over large statistical ensembles of ionic configurations, finding an increase in polarizability that is consistent with the level of discrepancy between theory and experiment.

Since the effects of temperature on the polarizability are relatively large (about 15% at 300 K), a measurement of polarizability in which the temperature is con-

trolled may allow one to observe a signature of the melting of a cluster. In this way, a polarizability experiment might complement that of the Freiburg group [15], who inferred the caloric curve of free sodium clusters in the size range  $N = 50$ –200 from the temperature dependence of the photofragmentation spectrum. They found cluster melting points that are not only lower than the bulk melting point, as expected for a finite system, but show an irregular variation with respect to cluster size that has still not been fully understood theoretically. We show here that a small, but in principle measurable, signature of melting may indeed be observed on the polarizability in some cases, offering the possibility of a very useful independent measurement of the cluster melting point.

We wish to consider sodium clusters up to a size  $N = 139$  and to construct large statistical ensembles of ionic configurations. To make this possible, we choose a simplified description [16] of the cluster, within density functional theory (DFT), in which the  $\text{Na}^+$  ions move classically on a potential-energy surface that we obtain by treating the delocalized valence electrons in the extended Thomas-Fermi (ETF) approximation. Exactly as in Ref. [16], our ETF approximation includes an exchange-correlation energy in the local-density approximation (LDA), a scaled Weizsäcker correction for gradient corrections to the electron kinetic energy, and a local pseudopotential to describe the electron-ion interaction; the computational cost of the method scales with system size as  $O(N \ln N)$ . We concentrate here on the experimentally accessible spherical average of the polarizability,  $\alpha = (\alpha_{xx} + \alpha_{yy} + \alpha_{zz})/3$ . We extract  $\alpha$  within the ETF approximation by a standard “finite-field” algorithm, applying an electric field  $\mathbf{F}$  to the cluster and inferring the components of the polarizability tensor from the induced dipole moment and, as a check, the coefficient of the quadratic term  $F^2$  in the total energy. The ionic coordinates are held fixed in each polarizability calculation for a given ionic configuration. This approximation is known to modify the polarizability at 0 K by about 1% [4,9] (at least for small clusters), and its effect on finite-temperature averages is thus expected to be similarly small. We choose an applied field step size of

TABLE I. Spherically averaged polarizabilities ( $a_0^3$ ) at 0 K calculated within the ETF approximation, using the “flat” pseudopotential of Ref. [16].

Na <sub>6</sub> <sup>a</sup>	Na <sub>7</sub> <sup>a</sup>	Na <sub>8</sub> <sup>a</sup>	Na <sub>20</sub> <sup>a</sup>	Na <sub>40</sub>	Na <sub>55</sub> <sup>a</sup>	Na <sub>93</sub>	Na <sub>139</sub>
634	672	765	1777	3356	4532	7600	10820

<sup>a</sup>Optimized geometries: Na<sub>6</sub>, pentagonal pyramid  $C_{5v}$ ; Na<sub>7</sub>, pentagonal bipyramid  $D_{5h}$ ; Na<sub>8</sub>, decahedral  $D_{2d}$ ; Na<sub>20</sub>, singly capped double icosahedron; Na<sub>55</sub>, double Mackay icosahedron.

0.0005–0.001 a.u. with five different field values in each of the  $x$ ,  $y$ , and  $z$  directions. Further, the real-space grid for the ETF solution was refined in such a way that purely numerical errors in the polarizability calculation are less than 1%.

Before discussing finite temperature, we shall first assess the ETF approximation for cluster polarizabilities at 0 K (see Table I). In the bulk limit  $N \rightarrow \infty$ , assuming a spherical geometry of radius  $R$ , one should expect to retrieve the classical result  $\alpha_{cl} = R^3$ . Such a trend is confirmed for our ETF polarizabilities in Fig. 1, where we have considered three possible definitions of  $R$  for a finite system of discrete ions:  $R_b = r_s N^{-1/3}$ , an “ionic” radius  $R_{ion}$ , and an “electronic” radius  $R_{el}$ , the latter two defined, respectively, in terms of the mean-square radii of the ionic and electronic distributions,  $R_{ion}^2 = 5/3 \langle r^2 \rangle_{ion}$  and  $R_{el}^2 = 5/3 \langle r^2 \rangle_{el}$ . Note that  $\alpha/R_b^3$  and  $\alpha/R_{ion}^3$  are each greater than unity, while  $\alpha/R_{el}^3$  is closer to unity for all  $N$ , consistent with the notion of an electron spillout.

The ETF polarizabilities are also in good general agreement with Kohn-Sham (KS) calculations taken from the literature for Na<sub>6</sub>–Na<sub>8</sub> and Na<sub>20</sub>, which are given in Table II together with some new calculations for this work using Gaussian basis-set orbitals [17,18]. As is apparent

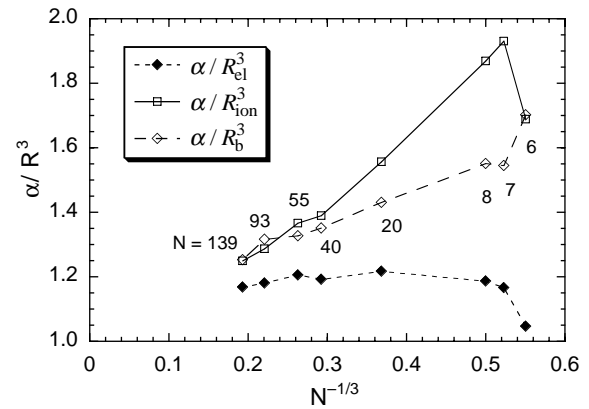


FIG. 1. Spherically averaged polarizabilities at 0 K calculated within the ETF approximation, scaled by three choices of  $R^3$  (see text).

from Table II, the recent literature for DFT-KS calculations shows a spread of values for polarizabilities of about 20% according to the choice of pseudopotential (or the use of all-electron methods) and the use of the LDA versus gradient-corrected exchange-correlation functionals (GGA). Some of this spread is simply due to the differing bond lengths assumed, as each author has relaxed the ionic structure in their chosen approximation. If in our own calculations, however, we freeze the bond lengths of Na<sub>8</sub> at those for the penultimate row of Table II, and perform all-electron calculations of the polarizability, we obtain  $\alpha = 732a_0^3$  (GGA-B3LYP),  $755a_0^3$  (GGA-PW91), and  $719a_0^3$  (LDA), a spread of 5% merely from differing choices of GGA or use of the LDA in the polarizability calculation. While the use of DFT thus necessarily leads to some uncertainty even at 0 K, we note that all theoretical

TABLE II. Spherically averaged polarizabilities ( $a_0^3$ ) at 0 K calculated within the KS approximation. Notation: “psp,” pseudopotential; “all,” all-electron; P86, B88-P86, B88-PW91, and B3LYP denote gradient-corrected exchange-correlation functionals using standard notation [18].

Author	Method	Na <sub>6</sub> <sup>a</sup>	Na <sub>7</sub> <sup>a</sup>	Na <sub>8</sub> <sup>a</sup>	Na <sub>20</sub> <sup>a</sup>
Moulet [3]	psp LDA	603	619	655	
Guan [4]	all LDA	612			
Rubio [5]	psp LDA			803	
Pacheco [6]	psp LDA			770	1830
Vasiliev [7]	psp LDA			794	
Calaminici [8]	all LDA	621	658	710	
Kümmel [9]	psp LDA	725		831	1980
Guan [4]	all P86	603			
Guan [4]	all B88-P86	640			
Rayane [10]	all B88-PW91	709	756	806	
Calaminici [8]	all B88-P86	682	722	775	
This work <sup>b</sup>	all B3LYP	646	688	741	1728
Expt. <sup>c</sup> [10]		754	808	901	2045

<sup>a</sup>Optimized geometries are as in Table I, except for Na<sub>20</sub>: double icosahedron minus one end cap plus two caps on waist.

<sup>b</sup>Basis set: 6-311G\* for structure relaxation, 6-311G\*\* (Na<sub>6</sub>–Na<sub>8</sub>) or 6-31G\* (Na<sub>20</sub>) for polarizability calculations.

<sup>c</sup>Experimental errors are estimated to be about 12%.

values in Table II are less than the corresponding experimental values (although some are contained within the experimental error bars of roughly 12% [10]).

Now let us turn to finite temperature. For this we shall take advantage of ETF molecular-dynamics (MD) trajectories, at closely spaced values of the (constant) total energy, that we used previously [19] to extract the ionic entropy of the cluster via a multiple-histogram analysis. Typically, we use MD runs of 50 ps for each total energy  $E$  (or split longer runs into 50 ps segments). Let  $\langle X \rangle_E$  be the time average, at energy  $E$ , of some property  $X(\{\mathbf{R}_I\})$  that depends on the ionic coordinates  $\{\mathbf{R}_I\}$ . Then the canonical average of  $X$  at temperature  $T$  is given by

$$\langle X \rangle_T = \int_{E_0}^{\infty} p(E, T) \langle X \rangle_E dE, \quad (1)$$

where  $p(E, T) = \Omega(E) \exp(-E/k_B T) / Z(T)$  is the usual Gibbs distribution for the probability of observing an energy  $E$  at temperature  $T$ ,  $\Omega(E)$  is the density of states obtained from the multiple-histogram analysis, and  $Z(T)$  is the normalizing canonical partition function. The thermal fluctuation  $\delta X^2 = \langle X^2 \rangle_T - \langle X \rangle_T^2$  of  $X$  may be obtained in a similar way, with  $\langle X^2 \rangle_T$  given by Eq. (1) with  $X$  replaced by  $X^2$ . The property  $X$  could be  $\alpha$ ,  $R_{\text{ion}}^3$ , or  $R_{\text{el}}^3$ . To illustrate this approach in practice, we show “raw” MD data for  $\alpha$  for  $\text{Na}_8$  in Fig. 2(a), where each point represents the time average of  $\alpha$  over an independent 50 ps MD run (there are 308 such points). The spread of values in the figure is a statistical effect due to the finite duration of this time average. After applying Eq. (1) to get the canonical average in Fig. 2(b), however, the data are automatically smoothed, since the integral acts as a weighted moving average.

Figure 3 shows the canonical averages of  $\alpha$ ,  $R_{\text{ion}}^3$ , and  $R_{\text{el}}^3$  calculated in this way for a range of cluster sizes, with each property scaled so that it is unity at  $T = 0$ . Note that the larger clusters considered here are singly charged, while a practical experiment would require a neutral cluster. However, we find less than 1% difference between *scaled* averages  $\langle \alpha \rangle_T / \langle \alpha \rangle_{T=0}$  for neutral and singly charged clusters for all temperatures  $T < 300$  K, when

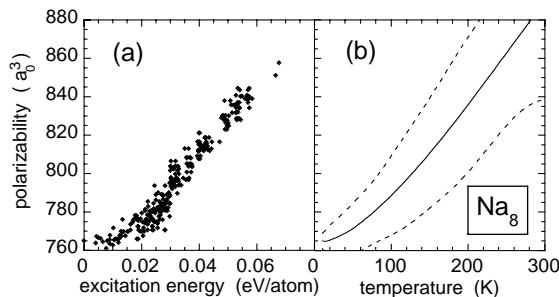


FIG. 2. Polarizability of  $\text{Na}_8$  in (a) microcanonical and (b) canonical ensembles (see text). The dotted lines in (b) indicate the intrinsic thermal fluctuation of the polarizability.

calculated for a given ensemble of ionic configurations. Our reason for considering singly charged clusters here is again to profit from large existing statistical ensembles of ionic configurations, with good statistics particularly in the important region of the solid-liquid transition.

The first point to note from Fig. 3 is that the simple estimates  $R_{\text{ion}}^3$  and  $R_{\text{el}}^3$  both overestimate the fractional increase of polarizability with temperature. The overestimate is rather large for small clusters, but as would be expected  $R_{\text{ion}}^3$  and  $R_{\text{el}}^3$  give better approximations to the temperature dependence as the cluster size increases, and  $R_{\text{el}}^3$  gives a slightly better approximation than  $R_{\text{ion}}^3$  for all  $N$ . The estimate  $R_{\text{ion}}^3$  is of particular interest, since it requires no electronic structure calculations and can thus be calculated with (computationally much cheaper) semiempirical interionic potentials. We note that, among the many approximations involved in taking  $R_{\text{ion}}^3$  and  $R_{\text{el}}^3$  as estimates of  $\alpha$ , there is an implicit assumption that all ionic configurations in the thermal ensemble are spherical. In fact, many deformed shapes contribute, and for these  $R^3$  does not give the polarizability even in classical electrostatics.

Second, at 300 K the polarizability is roughly 15% greater than its value at 0 K for all sizes studied here, an increase substantially greater than would be inferred from the bulk thermal expansivity ( $\sim 5\%$ ). This demonstrates

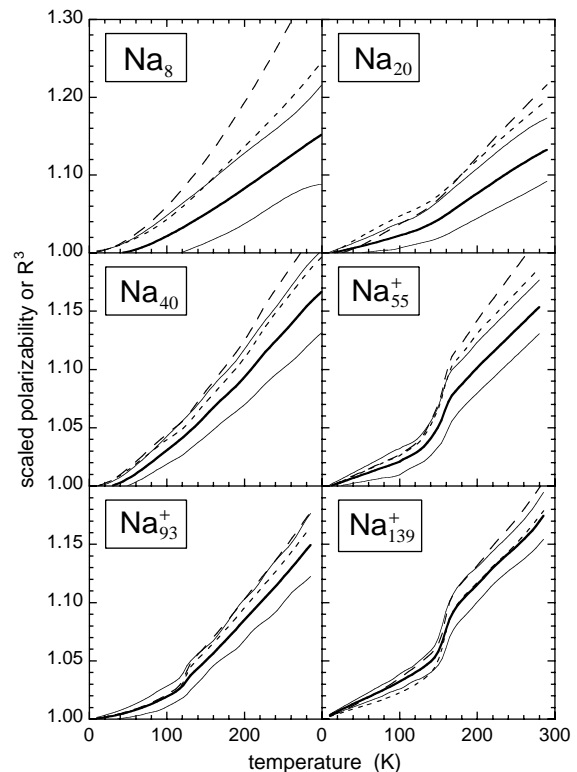


FIG. 3. Canonical average of polarizability  $\alpha$  (thick solid line),  $R_{\text{ion}}^3$  (long dashed line), and  $R_{\text{el}}^3$  (short dashed line) versus temperature. The thin solid lines show the thermal fluctuation ( $\pm$  one standard deviation) on  $\alpha$ . Each property is scaled by dividing by its value at 0 K.

the importance of the cluster surface, which comprises most of the atoms of the cluster even at a size of  $N = 139$ . A similar result has been found for  $\text{Na}_{20}$  in a tight-binding model [20]. This large increase in polarizability is consistent with the observed discrepancies between theory at 0 K and experiment apparent in Table II. However, both the polarizability at 0 K (calculated within DFT) and the experimental temperature of the clusters are subject to sufficient uncertainty at this point that it is difficult to make a precise quantitative comparison.

Finally, while the smaller clusters  $\text{Na}_8$ - $\text{Na}_{40}$  show a rather smooth increase of polarizability with temperature,  $\text{Na}_{55}^+$  and  $\text{Na}_{139}^+$  each show a distinct step in polarizability of about 5% at around 150 K, extending over a range of about 30 K. These steps correlate precisely with the solid-liquid transition of the cluster, studied in Ref. [19] within an identical ETF approximation. For instance, the canonical specific heat of  $\text{Na}_{139}^+$ , shown in Fig. 4, has a distinct peak at 155 K in the ETF approximation, which an inspection of ionic trajectories confirms as corresponding to the melting of the cluster [19]; the canonical specific-heat curves for the smaller clusters are much broader. The cluster  $\text{Na}_{93}^+$ , although possessing a fairly sharp melting transition at about 125 K, has a smaller polarizability step ( $\sim 1.5\%$ ) at this temperature. In all cases, a step in the polarizability correlates with similar steps in  $R_{\text{ion}}^3$  or  $R_{\text{el}}^3$ . The marked increase in cluster volume for  $\text{Na}_{55}^+$  and  $\text{Na}_{139}^+$  on melting is presumably because, in the ETF model, these systems exhibit compact low-temperature structures at or close to icosahedral shell closures. The structure for  $\text{Na}_{93}^+$ , by contrast, consists of surface growth on one side of an icosahedral core [19].

We should note that the melting point, which can be quite sensitive to the assumed interionic potential, is in the ETF model about two-thirds of the value measured by Schmidt *et al.* [15]. Thus, in a more realistic model the position of the step in the polarizability curve may be shifted, but we believe that the present ETF model gives a sufficiently good representation of the metallic bonding

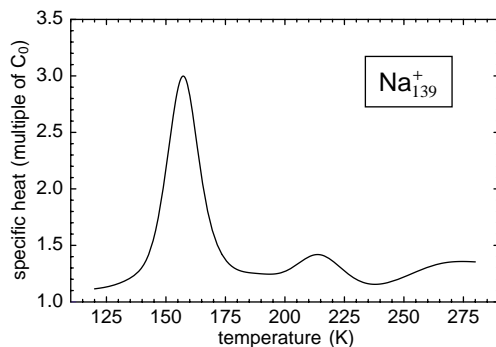


FIG. 4. Canonical specific heat of  $\text{Na}_{139}^+$  calculated within the ETF approximation (from Ref. [19]). The quantity  $C_0 = (3N - 9/2)k_B$  is the zero-temperature classical limit for the vibrational plus rotational specific heat.

of the cluster that the step will remain as a qualitative feature of the temperature dependence curve in any realistic model. (The melting point would also vary somewhat between charged and neutral clusters.) Moreover, the step for  $\text{Na}_{55}^+$  and  $\text{Na}_{139}^+$  is a sufficiently distinct feature of the temperature dependence curve that it would be experimentally detectable if the average polarizability at fixed temperature can be measured with sufficient precision, say, to better than about 2% in the vicinity of the solid-liquid transition. As noted in the introduction, this would provide a valuable independent measurement of the melting point. We hope that these comments offer an incentive to experimentalists to measure the temperature dependence of the polarizability.

R. Z. would like to acknowledge the support of IFC-PAR within the framework of Project No. 1901-01 between the CEA and the University of Pune, India.

- 
- [1] W.D. Knight, K. Clemenger, W.A. de Heer, and W.A. Saunders, *Phys. Rev. B* **31**, 2539 (1985).
  - [2] D.R. Snider and R.S. Sorbello, *Phys. Rev. B* **28**, 5702 (1983); W. Ekardt, *Phys. Rev. Lett.* **52**, 1925 (1984); D.E. Beck, *Phys. Rev. B* **30**, 6935 (1984).
  - [3] I. Moullet, J.L. Martins, F. Reuse, and J. Buttet, *Phys. Rev. Lett.* **65**, 476 (1990); *Phys. Rev. B* **42**, 11 598 (1990).
  - [4] J. Guan, M.E. Casida, A.M. Köster, and D.R. Salahub, *Phys. Rev. B* **52**, 2184 (1995).
  - [5] A. Rubio, J.A. Alonso, X. Blase, L.C. Balbás, and S.G. Louie, *Phys. Rev. Lett.* **77**, 247 (1996).
  - [6] J.M. Pacheco and J.L. Martins, *J. Chem. Phys.* **106**, 6039 (1997).
  - [7] I. Vasiliev, S. Ögüt, and J.R. Chelikowsky, *Phys. Rev. Lett.* **82**, 1919 (1999).
  - [8] P. Calaminici, K. Jug, and A.M. Köster, *J. Chem. Phys.* **111**, 4613 (1999).
  - [9] S. Kümmel, T. Berkus, P.-G. Reinhard, and M. Brack, *Eur. Phys. J. D* (to be published).
  - [10] D. Rayane *et al.*, *Eur. Phys. J. D* **9**, 243 (1999).
  - [11] E. Benichou *et al.*, *Phys. Rev. A* **59**, R1 (1999).
  - [12] R. Antoine *et al.*, *J. Chem. Phys.* **110**, 5568 (1999).
  - [13] T.P. Martin *et al.*, *J. Chem. Phys.* **100**, 2322 (1994); C. Ellert *et al.*, *Phys. Rev. Lett.* **75**, 1731 (1995); F. Chandezon *et al.*, *Chem. Phys. Lett.* **277**, 450 (1997).
  - [14] F. Chandezon, P. Dugourd, and M. Broyer (private communication).
  - [15] M. Schmidt *et al.*, *Phys. Rev. Lett.* **79**, 99 (1997); *Nature (London)* **393**, 238 (1998).
  - [16] P. Blaise, S.A. Blundell, and C. Guet, *Phys. Rev. B* **55**, 15 856 (1997).
  - [17] M.J. Frisch *et al.*, GAUSSIAN98, Revision A.7, Gaussian, Inc., Pittsburgh, 1998.
  - [18] J.B. Foresman and Æ. Frisch, *Exploring Chemistry with Electronic Structure Methods* (Gaussian, Inc., Pittsburgh, 1996), 2nd ed.
  - [19] P. Blaise, S.A. Blundell, and C. Guet (to be published).
  - [20] A. Bulgac and C. Lewenkopf, *Europhys. Lett.* **31**, 519 (1995).